JCI The Journal of Clinical Investigation

The estrogen signaling pathway reprograms prostate cancer cell metabolism and supports proliferation and disease progression

Camille Lafront, … , Éric Lévesque, Étienne Audet-Walsh

J Clin Invest. 2024. https://doi.org/10.1172/JCI170809.

Research In-Press Preview **Endocrinology** **Oncology**

Just as the androgen receptor (AR), the estrogen receptor α (ERα) is expressed in the prostate and is thought to influence prostate cancer (PCa) biology. Yet, the incomplete understanding of ERα functions in PCa hinders our ability to fully comprehend its clinical relevance and restricts the repurposing of estrogen-targeted therapies for the treatment of this disease. Using two human PCa tissue microarray cohorts, we first demonstrated that nuclear ERα expression was heterogeneous among patients, being only detected in half of tumors. Positive nuclear ERα levels were correlated with disease recurrence, progression to metastatic PCa, and patient survival. Using in vitro and in vivo models of the normal prostate and PCa, bulk and single-cell RNA-Seq analyses revealed that estrogens partially mimic the androgen transcriptional response and induce specific biological pathways linked to proliferation and metabolism. Bioenergetic flux assays and metabolomics confirmed the regulation of cancer metabolism by estrogens, supporting proliferation. Using cancer cell lines and patient-derived organoids, selective estrogen receptor modulators, a pure anti-estrogen, and genetic approaches impaired cancer cell proliferation and growth in an ERα-dependent manner. Overall, our study revealed that, when expressed, ERα functionally reprograms PCa metabolism, is associated with disease progression, and could be targeted for therapeutic purposes.

The estrogen signaling pathway reprograms prostate cancer cell metabolism and supports proliferation and disease progression

Camille Lafront[1,2,3], Lucas Germain[1,2,3], Gabriel H. Campolina-Silva[4,5], Cindy Weidmann[2,3], Line Berthiaume[2,3], Hélène Hovington[3,6], Hervé Brisson[3,6], Cynthia Jobin[1,2,3], Lilianne Frégeau-Proulx[1,2,3], Raul Cotau[2,3,7], Kevin Gonthier[1,2,3], Aurélie Lacouture[1,2,3], Patrick Caron[2,3], Claire Ménard[6], Chantal Atallah[6,8], Julie Riopel[2,8], Éva Latulippe[8], Alain Bergeron[3,7,9], Paul Toren[3,7,9], Chantal Guillemette[2,3,10], Martin Pelletier[11,12,13], Yves Fradet[3,7,9], Clémence Belleannée[4,5], Frédéric Pouliot[3,7,9], Louis Lacombe[3,7,9], Éric Lévesque[2,3,6], and Étienne Audet-Walsh*[1,2,3]

Affiliations

[1]Department of Molecular Medicine, Université Laval, Quebec City, Canada

[2]Endocrinology and Nephrology Division, CHU de Québec-Université Laval Research Center (CRCHUQ-UL), Quebec City, Canada

[3]Cancer Research Center (CRC) of Université Laval, Quebec City, Canada

[4]Department of Obstetrics, Gynecology and Reproduction, Université Laval, Quebec City, Canada

[5]Reproduction, Mother and Youth Health Division, CRCHUQ-UL, Quebec City, Canada

[6]Department of Medicine, Université Laval, Quebec City, Canada

[7]Oncology Research Division, CRCHUQ-UL, Quebec City, Canada

[8]Department of Pathology, CHU de Québec-Université Laval, Quebec City, Canada

[9]Department of Surgery, Université Laval, Quebec City, Canada

[10]Faculty of pharmacy, Université Laval, Quebec City, Canada

[11]Department of Microbiology-Infectious Diseases and Immunology, Université Laval, Quebec City, Canada

[12]Infectious and Immune Diseases Research Division, CRCHUQ-UL, Quebec City, Canada

[13]ARThrite Research Center, Université Laval, Quebec City, Canada

The authors have declared that no conflict of interest exist.

*** Corresponding Author:** Étienne Audet-Walsh, Centre de recherche du CHU de Québec, 2705 Boulevard Laurier, room R-4714, Québec City, QC, Canada, G1V 4G2

Phone: 1-418-525-4444 ext. 48678 ; e-mail : etienne.audet-walsh@crchudequebec.ulaval.ca

ABSTRACT

Just as the androgen receptor (AR), the estrogen receptor α (ERα) is expressed in the prostate and is thought to influence prostate cancer (PCa) biology. Yet, the incomplete understanding of ERα functions in PCa hinders our ability to fully comprehend its clinical relevance and restricts the repurposing of estrogen-targeted therapies for the treatment of this disease. Using two human PCa tissue microarray cohorts, we first demonstrated that nuclear ERα expression was heterogeneous among patients, being only detected in half of tumors. Positive nuclear ERα levels were correlated with disease recurrence, progression to metastatic PCa, and patient survival. Using in vitro and in vivo models of the normal prostate and PCa, bulk and single-cell RNA-Seq analyses revealed that estrogens partially mimic the androgen transcriptional response and induce specific biological pathways linked to proliferation and metabolism. Bioenergetic flux assays and metabolomics confirmed the regulation of cancer metabolism by estrogens, supporting proliferation. Using cancer cell lines and patient-derived organoids, selective estrogen receptor modulators, a pure anti-estrogen, and genetic approaches impaired cancer cell proliferation and growth in an ERα-dependent manner. Overall, our study revealed that, when expressed, ERα functionally reprograms PCa metabolism, is associated with disease progression, and could be targeted for therapeutic purposes.

INTRODUCTION

Prostate cancer (PCa) is the most common cancer for men in 112 countries (1). This disease is highly dependent on the androgen receptor (AR), a transcription factor that modulates several biological pathways essential for the growth and survival of PCa cells. Notably, AR regulates cancer cell metabolism to synthesize energy, such as promoting glycolysis, mitochondrial respiration, and fatty acid β-oxidation, as well as inducing cancer cell proliferation (2-5). This dependency of PCa cells on AR activity is the reason why hormonal therapies used to treat PCa either target the production of these hormones through androgen deprivation therapies (ADTs), or the AR signaling pathway using anti-androgens (2, 5). Tumor cells initially respond favorably to these treatments but inevitably evolve to the life-threatening form of the disease named castration-resistant PCa (CRPC) (2, 5, 6); therefore, there is an urgent need to find new therapeutic targets to treat this lethal disease.

In addition to androgens, estrogens, notably the most potent endogenous estrogen estradiol (E_2), can also modulate PCa cell biology (as reviewed in (7-9)). For example, the combination of both androgens and estrogens is essential for the induction of prostate carcinogenesis in preclinical models (10-13). Moreover, mice knockout (KO) for *Cyp19a1*, which encodes the aromatase enzyme essential for estrogen biosynthesis, failed to develop PCa despite exhibiting increased androgen production (14). Mice with aromatase overexpression, which leads to an increase of the estrogens/androgens ratio, do not develop PCa either (15). In addition, plasma E_2 levels were positively correlated with high-grade PCa (16) and, in patients under ADTs, with evolution to CRPC (17). Consequently, all these data suggest that the estrogen signaling pathway is as important as the androgen pathway for PCa biology.

The effects of estrogens on prostate cells are thought to be mostly mediated by the estrogen receptors ERα and ERβ (8). They are both transcription factors of the nuclear receptor family like

AR, however with opposite effects in the prostate. ERβ is thought to be a tumor suppressor (18-20), whereas ERα is associated with oncogenic functions (10, 21, 22). In vivo models support an oncogenic role for ERα, as its genetic ablation in mouse models blocks the initiation of PCa following testosterone + E_2 treatment (8). Conversely, mice that no longer express ERβ (βERKO) exhibit increased hyperplasia and androgen signaling (20). Thus, the oncogenic effects of E_2 in the prostate are likely conducted through the activation of ERα.

Considering these data, ERα represents a potentially effective therapeutic target in PCa. One of the very first ADTs was to give high doses of estrogens to patients, which generate a negative feedback loop in the hypothalamic–pituitary–testicular axis and thus induce a pharmacological castration (2). However, this approach was not intended to directly target ERα's action in the prostate. To target ERα and the "endogenous" estrogen signaling pathway, as opposed to high exogenous estrogen doses, many drugs are currently available to inhibit the action of this receptor in the context of ERα-positive breast cancer (23), namely selective estrogen receptor modulators (SERMs). Several studies have attempted to evaluate the efficacy of SERMs in different clinical settings, such as treating high-grade prostate intraepithelial neoplasia (HGPIN) to prevent PCa recurrence following surgery, treating treatment-naïve bone metastatic PCa, or treating CRPC. However, conflicting results were obtained, with either positive responses (24-26) or no significant changes (27-29). In these studies, no stratification of PCa patients was performed based on the presence or absence of ERα prior to SERMs' testing, possibly explaining such conflicting results. Another limitation of using SERMs to treat PCa is our limited understanding of the role of ERα as a transcription factor in the prostate and PCa, given notably that the most commonly used PCa cell lines do not express ERα, or express a mutated AR that can be activated by E_2 (*e.g.,* LNCaP cells; (2, 7)).

In this study, our objective was to elucidate the role of estrogens, and particularly of ERα, in the biology of PCa. We first used a clinically validated approach (that is normally used for breast cancer) to determine the expression of ERα in PCa samples. Despite its heterogeneity, the expression of ERα positively correlated with more aggressive prostate tumors and clinical progression. We then used in vivo preclinical mouse models (WT and PCa), human PCa cell lines and patient-derived organoids (PDOs) to study the cellular impacts of modulating the estrogen signaling pathway in PCa. We observed that hundreds of genes were differentially expressed, both in vitro and in vivo, and highlighted that reprogramming of cancer cell metabolism was a major function of ERα in PCa, supporting the aberrant proliferation of these cancer cells. Finally, we demonstrated in preclinical models that, when ERα is expressed, SERMs can be used as efficient therapeutic agents against ERα-expressing prostate tumors.

RESULTS

ERα expression is heterogeneous in PCa and, when expressed, is associated with a more aggressive disease

We first studied ERα total protein levels by reanalyzing proteomics data from the TCGA consortium (the prostate adenocarcinoma [PRAD] dataset) (30, 31), with its protein levels separated as low versus high. High ERα protein levels were associated with a shorter biochemical recurrence (BCR)-free survival rate, the first indication of PCa progression following surgery (Figure 1A). In patients with BCR, 42% had high ERα protein levels compared to 21% in patients without BCR (Figure 1B; p=0.002). Despite associating ERα total protein levels with BCR, proteomics analyses did not distinguish between ERα levels in the different cells from the tumor microenvironment, nor distinguish between active (nuclear) or inactive (cytoplasmic) receptors.

Consequently, we then performed an immunohistochemistry study of ERα in human PCa samples, similar to what is routinely performed for breast cancer. Indeed, in the breast cancer field, the expression pattern of ERα is first evaluated before prescribing (or not) hormonal therapies. To determine if such a clinical trajectory could be translated to PCa, we then investigated the expression profiles of ERα in prostate tumors using the clinical pipeline for defining ERα expression status in breast cancer at our local hospital, using a clinically validated antibody for this receptor (clone EP1, Dako). The specificity of the ERα antibody was further confirmed using the established breast cancer cell lines MCF7 (ERα-positive) and MDA-MB-231 (ERα-negative) (Supplemental Figure S1A). ERα expression levels were then studied in an established prostate tissue microarray (TMA) comprising tissues from 239 patients (see Supplemental Table S1 for cohort description) (32, 33).

First, expression of ERα in human PCa was highly heterogeneous between tumors, being either absent or present in nuclei, cytoplasm and/or stroma (Figure 1C and Supplemental Figure S1, B-E). ERα staining was stronger in stromal cells, as reported previously (34-36), being high in 70% of the samples (Supplemental Figure S1F). Less studied in cancer cells due to lower expression, positive nuclear ERα staining in cancer cells, indicative of an activated receptor, was detected in 51% of patients' tumors (Supplemental Figure S1F). Following radical prostatectomy, nuclear ERα positivity was associated with a shorter BCR-free survival rate (log-rank *p*-value of 0.006; Figure 1D). Indeed, 61% of patients with BCR had positive ERα nuclear expression, compared to 45% in patients without BCR (Figure 1E; $p<0.001$). In univariate Cox regression analyses, positive ERα nuclear levels were associated with a HR of 1.94-fold higher risk of BCR following surgery compared to negative ERα nuclear levels (Figure 1F; left). Importantly, this association between nuclear ERα (active) status and BCR remained significant when the model was adjusted for other variables associated with BCR in multivariate analyses, such as Gleason score, tumor stage, prostate-specific antigen (PSA) levels at diagnosis, nodal invasion status, and surgical margins (HR for positive nuclear ERα: 3.02; Figure 1F; right). On the contrary, cytoplasmic and stromal positivity for ERα was not significantly associated with a BCR-free survival rate (Supplemental Figure S1, G-H).

Next, we validated these results in an independent dataset, comprised of 41 patients who received neoadjuvant ADTs before surgery (with 32 patients out of 41 who received both ADT and anti-androgens; cohort description in Supplemental Table S2). Consequently, even though these patients did not have a "clinical CRPC" at surgery, the studied samples were comprised of cancer cells surviving castration and evolving to lethal CRPC. In this cohort, ERα was quantified using the same pipeline and threshold established for the discovery cohort, again by reviewers blinded to

clinical data. In this setting, nuclear ERα protein detection was positive in 54% of the samples (22/41; Figure 1G and Supplemental Figure S1, I-J). In this dataset, which is representative of more aggressive tumors, most patients experienced BCR (>60%). Importantly, positive nuclear ERα expression was significantly associated with faster time to metastasis and decreased overall patient survival (Figure 1, H-I; multivariate analyses using Cox regressions were not performed due to the lack of statistical power). This cohort allows us to link nuclear ERα expression in cancer cells with the evolution to lethal CRPC.

As seen in the discovery cohort, stromal ERα levels were much higher compared to the epithelial/tumoral compartment but were again not associated with disease progression in survival analyses (Supplemental Figure S1, K-L). These results, even though stromal ERα is most probably important in PCa biology (see Supplemental Discussion), led us to focus our investigation on the functional role of ERα specifically in cancer cells and the epithelial compartment.

Overall, using a clinically validated ERα antibody in two TMAs, these results first indicate that ERα expression is heterogeneous between patients and that it is not expressed in all tumors. Consequently, if a patient is given any ERα-targeted therapy, its expression in cancer cells should first be validated. Secondly, when expressed, often a low percentage of cells are positive for ERα (>1-10%). Yet, positive nuclear (active) ERα levels were significantly associated with PCa progression following prostatectomy, and even so in patients' tumors under neoadjuvant ADTs in relation to metastases and overall survival. Together, these results confirm that ERα can be expressed in human prostate tumors and suggest that ERα-positive or ERα-negative status may apply to PCa tumors and be pertinent for prognosis and repurposing of anti-estrogens.

Modulation of the normal mouse prostate transcriptome in vivo by androgens and estrogens

To gain preliminary insights into ERα influence on PCa biology, we first sought to determine the ERα transcriptome in the normal prostate. Mouse studies showed that ERα-positive cells are widely distributed throughout the prostate epithelium, albeit at higher percentages in the anterior and dorsolateral prostate lobes (>75% ERα-positive cells) than in the ventral prostate (37% ERα-positive cells) (Figure 2, A-B). Staining intensity was also studied as an indirect indicator of the relative amount of nuclear ERα positivity per epithelial cell and showed a similar pattern between the lobes (>60% intensity in both the anterior and dorsolateral lobes, versus around 30% intensity in the ventral prostate). Irrespective of the prostate lobe, ERα staining was mostly nuclear.

Since androgens can be converted into estrogens with aromatase, it is reasonable to investigate the estrogen signature in parallel with androgens effects. To this end, mice were first castrated to inhibit both androgen and estrogen production by the testes. After 72h to ensure steroid deprivation, animals were then treated for 24h with the vehicle, testosterone, E_2 or both hormones, to study the androgen and the estrogen transcriptional signatures in vivo in the normal prostate. In this short-term setting (similar to the settings defined by Pihlajamaa *et al.* to study the androgen response (37)), the prostate weight was not altered after four days post-castration (Supplemental Figure S2A), as opposed to the long-term impact of castration that normally leads to >90% decrease in prostate weight (38). Given that the estrogen transcriptional response was, to the best of our knowledge, never defined neither in the normal prostate nor in PCa, we then performed RNA-Seq analyses using this experimental design. Firstly, in the WT mouse prostate, treatment with testosterone was found to alter the expression of 696 genes (Figure 2C). In parallel, E_2 led to the significant modulation of 436 genes (Figure 2C). Interestingly, activation of both pathways simultaneously yielded the greatest transcriptional response, with 1,086 and 1,059 genes up- and

downregulated, respectively (Figure 2C). All significantly modulated genes by each treatment are listed in Supplemental Table S3.

To identify the biological pathways regulated by androgens, estrogens, or both, we performed Gene Set Enrichment Analysis (GSEA; Figure 2, D-H, and Supplemental Figure S2, B-D). As expected, activation of AR by testosterone induced a transcriptional response linked to the androgen response, as well as activating key oncogenic pathways in PCa (4, 39), including the mTORC1 and MYC signaling pathways (Figure 2, D-E, and Supplemental Figure S2B). Testosterone also upregulated pathways linked to cell metabolism in the normal prostate, inducing genes associated with oxidative phosphorylation (OXPHOS) and glycolysis, the two major pathways leading to ATP synthesis (Figure 2, D and F, and Supplemental Figure S2C). In addition, pathways linked to lipid metabolism were enriched, such as fatty acid metabolism and adipogenesis (Figure 2D), as reported previously in the mouse prostate (37). Overall, AR activation in the normal prostate induced pathways associated with proliferation and metabolism.

Interestingly, treatment with E_2 induced a transcriptional signature generally similar to the androgen-dependent signature, notably upregulating genes linked to protein synthesis and cellular proliferation such as the mTORC1 and MYC signaling pathways (Figure 2G and Supplemental Figure S2D). E_2 also induced specific pathways not targeted by androgens in the prostate, such as the cholesterol homeostasis signature, KRAS activation, and pathways related to immunity and angiogenesis (Figure 2, G-H). Even though testosterone could be aromatized into E_2, the small overlap between genes regulated by these two individual treatments suggests that minimal aromatization, if at all, occurred during the 24h treatment timeframe of the current study (Figure 2I). Indeed, the circulating hormone levels in mice 24h after injection of testosterone, E_2, or both, clearly showed specific hormonal exposure (Supplemental Figure S2E).

The combination of both hormones further increased the total transcriptional regulation (Figure 2C and 2I), but most of these modulated genes were part of the same biological pathways already enriched by individual treatment, such as upregulation of the mTORC1 and MYC signaling pathways as well as a strong metabolic signature (Supplemental Figure S2, F-G). Quantitative real-time reverse-transcription (qRT)-PCR confirmed the enrichment of metabolic genes following all three hormonal combinations (Supplemental Figure S2H).

Of note, the GSEA early and late estrogen response gene signatures, established using mostly breast cancer models (40), were not significantly modulated by E_2 in the normal prostate. As such, these results suggest that the transcriptional response modulated by estrogens is distinct between the normal prostate and the classic "estrogen response" transcriptional signatures. To confirm this supposition, we compared the top 300 identified estrogen-responsive genes in the MCF7 breast cancer model (41) with the estrogen-responsive genes identified herein in the mouse prostate, and observed little overlap with only 15/300 genes (5%) common to both lists (Figure 2J). In these 15 genes, well-known ERα target genes were identified, such as *Greb1* and *Pgr*, being also positively regulated by estrogens in the prostate (Figure 2K). Comparison with a second estrogen-treated MCF7 dataset (42) also indicated very few shared genes shared with the mouse prostate's estrogen response (Supplemental Figure S2I).

Overall, these results show that, in the normal mouse prostate, E_2 stimulation leads to a distinct transcriptional signature from the "classic" estrogen response that partially mimics androgen stimulation by promoting biological pathways linked to cell proliferation and metabolism.

Reprogramming of the mouse PCa transcriptome in vivo by androgens and estrogens

After defining the estrogen transcriptional response in the normal prostate, we then studied this hormonal response in an established transgenic mouse model that develops PCa (C57BL/6J PB-Cre4$^{+/-}$;*Pten*$^{fl/fl}$) (Figure 3A; left) (43). Most tumor cells had strong nuclear AR expression (Figure 3A middle, and Supplemental Figure S3A). As observed in human samples (Figure 1), nuclear ERα expression was heterogenous in mouse tumors (Figure 3A right, and Supplemental Figure S3A). Compared to the normal prostate, the number of nuclear ERα-positive cells in murine tumors remained mostly the same, being only slightly increased in the dorsolateral lobes (Supplemental Figure S3B). However, given increased cellularity within tumors, total ERα levels were higher, as shown by Western blot analyses (Figure 3B).

We next proceeded to bulk RNA-Seq experiments in this PCa mouse model with a similar methodology as previously described (37). Testosterone treatment modulated the expression of 1,746 genes (Figure 3C); that is 2-fold more genes than observed in the normal prostate (Figure 2C). In the case of E_2, a total of 957 genes were significantly modulated (Figure 3C), which is again 2-fold more than in the normal prostate (Figure 2C) and correlates with increased ERα expression in prostate tumors. Hormonal co-treatment induced the greatest transcriptional response with the modulation of a total of 2,691 genes (Figure 3C). All significantly modulated genes by each treatment are compiled in Supplemental Table S4.

Secondly, GSEA analyses were performed to highlight the biological pathways regulated by androgens and estrogens. The activation of AR in PCa induced similar gene signatures than in the normal prostate, such as the androgen response, MYC targets, mTORC1 signaling, and the metabolic gene signatures OXPHOS and fatty acid metabolism (Figure 3, D-E, and Supplemental

Figure S3, C-E). Some new gene signatures specifically regulated in mouse PCa were observed, such as cholesterol homeostasis.

Like androgens, multiple oncogenic pathways were found to be induced by estrogens, such as the mTORC1 signaling, MYC targets, cholesterol homeostasis, and reactive oxygen species (ROS) pathways (Figure 3, F-H, and Supplemental Figure 3, C-E), which were also similarly induced in the normal prostate (Figure 2, G-H). Notably, the OXPHOS pathway was upregulated (Figure 3I), which was not found to be enriched by estrogens in the normal prostate (Figure 2G).

Finally, as observed in the normal mouse prostate, the combination of testosterone + E_2 led to a stronger transcriptional response (Figure 3, C and H), while stimulating mostly the same gene signatures as individual treatments such as OXPHOS, MYC targets, mTORC1 signaling, and fatty acid metabolism (Supplemental Figure S3, C-F). Altogether, these results indicate that both androgens and estrogens have a major impact on the mouse PCa transcriptome in vivo.

Furthermore, E_2 treatment strongly induced the well-known ERα target genes *Greb1* and *Pgr* (Figure 3J), along with metabolic genes (Figure 3K). Most of the estrogenic response in this mouse PCa model was distinct from the "classic" estrogen response, with less than 11% overlap with the MCF7 estrogen response (Supplemental Figure S3, G-H). Clearly, the estrogen transcriptome is distinct in breast cancer compared to the one in the prostate and PCa; yet, the prostate-specific estrogen signature showed an important intersection between the mouse prostate and PCa tissues, with an overlap of 63% of estrogen-responsive genes (Supplemental Figure S3I).

Given that the prostate exhibits complex cell populations (38), we next wanted to better identify the estrogenic signature in the epithelial/tumoral component using the prostate-specific *Pten* KO model. To this end, single-cell RNA-Seq was performed in PCa-developing mice with and without 24-hour treatment with E_2. As expected, an important diversity of cell types was

detected, including various epithelial cell populations, mesenchymal/stromal cell subgroups, and immune cell types (Supplemental Figure S4A). These cell subtypes were identified with specific markers described by Karthaus and colleagues (38), such as *Epcam* and *Krt8* for epithelial, *Krt5* for basal, and *Col5a2* and *Rspo3* for mesenchymal/stromal compartment (Supplemental Figure S4, B-F). *Esr1*, encoding for ERα, was detected in mesenchymal (stromal) cells (Supplemental Figure S4G), consistent with high protein levels in the stroma (Figure 1 and Supplemental Figure S1). Importantly, *Esr1* was also expressed in epithelial cells expressing epithelial luminal markers, such *Pbsn* and *Krt8* (Figure 3L, and Supplemental Figure S4, D and G-H). These *Pbsn*-positive cells (Supplemental Figure S4H), corresponding to luminal cells actively secreting prostatic fluid as well as the tumoral compartment with directed *Pten* deletion in this PCa mouse model, exhibited the modulation of 138 genes following E_2 stimulation, notably the induction of *Greb1* (Figure 3M and Supplemental Figure S4, I-J). Of note, *Esr2*, encoding for ERβ, was undetectable in almost all cell types analyzed (Supplemental Figure S4K). Then, we performed GSEA analyses to study the estrogenic response in these *Pbsn*-positive cells, highlighting OXPHOS as the major pathway enriched following E_2 treatment (Figure 3, N-O), as well as other pathways promoting proliferation like MYC targets and fatty acid metabolism (Figure 3O, and Supplemental Figure S4L). Altogether, these results confirm that *Esr1* (ERα) is expressed both in the stromal and epithelial/tumor components of the prostate, and that, importantly, estrogens induce a metabolic gene signature in the epithelial/tumor compartment.

Functional reprogramming of human PCa cell metabolism by estrogens

We then assessed the estrogenic response in human PCa cell lines. Given the usage of non-specific antibodies (7, 44, 45), conflicting reports were published regarding ERα and ERβ

expression status in human in vitro PCa models. Consequently, we first verified the expression of both ERs in commonly used PCa cell lines using validated antibodies with appropriate controls such as ERα-positive (MCF7) and negative (MCF10A) cell lines (Figure 4A). The majority of PCa cell lines tested did not express detectable/high protein levels of ERα, except VCaP cells. After longer film exposure, ERα expression was also detected in PC3 cells, but at really low levels (data not shown and (7)). AR status of PCa cell lines could be clearly distinguished. ERβ expression was also evaluated with the antibody CWK-F12 (DSHB), validated for its specificity (44), but none of the cell lines tested displayed detectable protein levels (data not shown). As such, the heterogeneous expression of ERα observed in PCa cell lines partially mimics the heterogeneity previously observed in patients (Figure 1).

Since VCaP expressed both AR and ERα, this human PCa cell line was used to study the estrogen transcriptional response by RNA-Seq. It must be noted that VCaP cells were isolated from a vertebrae metastasis of a patient after his cancer became resistant to ADTs and the anti-androgen flutamide; thus, this in vitro model was established, by definition, from a CRPC tumor (2, 46). After steroid deprivation for 48h, VCaP cells were treated for 24h with the synthetic androgen R1881, E_2, or a combination of both, before RNA-Seq analyses (all significantly modulated genes are listed in Supplemental Table S5). AR activation induced a strong androgen response, as well as regulated multiple pathways linked to cell proliferation and metabolism, notably the mTORC1 signaling, the OXPHOS gene signatures, and the cholesterol homeostasis signature (Figure 4, B-C, and Supplemental Figure S5, A-B). Most of the regulated pathways were also observed in vivo in the normal mouse prostate (Figure 2) and in mouse PCa (Figure 3).

Multiple pathways regulated by E_2 in VCaP cells were also shared with those induced by estrogens in mouse tumors. Indeed, signaling pathways linked to proliferation (MYC targets, G2M

checkpoint), protein regulation (unfold protein response [UPR] and mTORC1 signaling), and cholesterol homeostasis were upregulated following hormonal treatment (Figure 4D and Supplemental Figure S5, A and C-D). Particularly, estrogens enriched the OXPHOS pathway in VCaP cells (Figure 4, D-E), as seen in vivo in mouse PCa (Figure 3) but not in the normal prostate (Figure 2). Finally, the androgen response, a tumorigenic pathway in VCaP cells, was also enriched with estrogens (Figure 4, D and F). Genes comprised in this pathway notably include *KLK3*, encoding for the PSA, which was significantly upregulated following each hormonal treatment (Figure 4C, right). This indicates that E_2, just as androgens, has oncogenic functions in this cell line. As observed in vivo, the combination of both hormones led to the enrichment of the same observed pathways as in individual treatments (Supplemental Figure S5, A and E-F). Altogether, these results confirm that E_2 treatment induces a major transcriptional response in PCa cells, promoting oncogenic pathways and inducing metabolic genes important for PCa biology, such as mitochondrial respiration (OXPHOS).

We next interrogated the functional impacts of this transcriptional signature on cancer cell biology. As previously reported (47), E_2 significantly stimulated VCaP cell proliferation (Figure 4G and Supplemental Figure S5G). Importantly, in this cell line that exhibits high AR dependency (2), the impact of E_2 on proliferation was as strong as R1881. Note that other human PCa cell lines that do not express ERα did not show any significant modulation by both E_2 and PPT (a specific agonist of ERα), irrespective of their AR status (such as DU145, 22Rv1, and LAPC-4 cells, see Supplemental Figure S5H and (7)). We next wanted to validate that E_2 not only regulates the expression of genes associated with OXPHOS, but that it also functionally regulates mitochondrial activity. To do so, oxygen consumption rates (OCR) of treated-VCaP cells were measured during a mitochondrial stress test (Figure 4H). As predicted from RNA-Seq, both androgens and estrogens

induced basal and maximal respiratory capacities of VCaP cells. Indeed, E_2 treatment induced mitochondrial DNA content (Supplemental Figure S5I). The usage of PPT also confirmed that this estrogenic regulation of mitochondrial respiration was ERα-dependent. On the contrary, the knockdown of *ESR1* with siRNAs abolished the E_2-mediated induction of mitochondrial activity, further validating the specificity of this hormonal response (Supplemental Figure S5, J-K). Finally, the co-activation of both receptors also led to a significant increase in basal and maximal cell respiration compared to the control condition, although the effect of the co-treatment was not additive and led to a smaller induction of OCR compared to androgens alone.

To further decipher the metabolic impacts of androgens and estrogens, metabolomics analyses were performed. Firstly, the fate of pyruvate, the main product of glycolysis, was studied. Once synthesized, pyruvate can be converted into the amino acid alanine or be used to produce ATP, either through lactate synthesis or by directly fueling the TCA cycle that supports mitochondrial respiration (Figure 5A). Regardless of the hormonal treatment, alanine (Figure 5B, left), lactate (Figure 5B, right), and TCA cycle intermediates (Figure 5C), including citrate and malate, were all increased following AR or ERα activation. The observations that the levels of all TCA cycle intermediates measured were increased following treatment with E_2 or R1881 (Figure 5C), thus fueling the electron transport chain to support mitochondrial respiration (Figure 4), are consistent with RNA-Seq results (Figure 3-4). Interestingly, stable isotope tracer analyses using ^{13}C-labelled glucose confirmed increased metabolic fluxes through aerobic glycolysis (lactate; Figure 5D; left), alanine synthesis (Figure 5D; right), and TCA cycle activity (Figure 5E), with E_2 and R1881 both significantly inducing ^{13}C-enrichment of downstream intermediates. Some differences were observed, but mostly regarding the fold increase in metabolite levels. For example, androgens induced alanine levels by more than 5-fold compared to vehicle, as opposed

to E_2 which was over 2-fold (Figure 5B; right) and consistent with a smaller flux of ^{13}C from glucose into alanine (Figure 5D; right). These results show that E_2 stimulation promotes PCa cell metabolism, notably by increasing glucose consumption and usage in cancer cells, as observed following AR activation. As such, we hypothesized that the E_2-dependent metabolic program was essential for the E_2-dependent activation of proliferation. Indeed, treatment with metformin, an inhibitor of mitochondrial respiration (48), significantly impaired the E_2-mediated increase in proliferation, demonstrating that regulation of bioenergetic pathways by estrogens is essential to promote maximal cancer cell proliferation (Figure 5F).

Another important pathway induced at the mRNA level was the mTORC1 pathway, often associated with protein synthesis, which requires energy and amino acids. Accordingly, all hormonal treatments significantly induced most detectable amino acids, including glutamate, asparagine, cysteine, proline, and aspartate (Figure 5G). Consequently, both androgens and estrogens promoted ATP-generating pathways, namely aerobic glycolysis and mitochondrial respiration, as well as stimulated biomass production through increased amino acid levels. In line with this hypothesis, E_2 stimulation activated the mTOR signaling pathway, as shown by phosphorylation of its downstream targets S6 and S6K (Figure 5H), which is similar to the results obtained following AR activation (Figure 5H and as described previously (4, 49)).

Impact of anti-estrogen treatments in ERα-positive PCa

Next, we wanted to determine if targeting ERα could block the metabolic and proliferative impacts of estrogens in PCa by using ERα-positive breast cancer drugs, such as the pure anti-estrogen fulvestrant and SERMs (tamoxifen, raloxifene and toremifene). We performed a mitochondrial respiration study, with SERMs or fulvestrant co-treated with estrogens (Figure 6A).

As expected, E_2 significantly increased the respiratory capacities of VCaP cells and, importantly, tamoxifen, raloxifene, toremifene, and fulvestrant were able to impair or completely block this induction of mitochondrial capacities (Figure 6A). In line, treatments with SERMs or fulvestrant blocked the E_2-mediated stimulation of PCa cell proliferation (Figure 6B), consistent with an ERα-specific response as shown using siRNAs against *ESR1* (Supplemental Figure S5I). Moreover, co-treatment with fulvestrant impaired the E_2-dependent transcriptional regulation in VCaP cells, as validated by qRT-PCR (*PGR*, *E2F1, BRCA1*, and *KLK3*; Supplemental Figure S6A). Furthermore, co-treatment with fulvestrant only blocked the E_2-mediated increase in respiration and proliferation, without impacting the AR-dependent effects (Figure 6C and Supplemental Figure S6B). Similarly, treatment with the anti-androgen enzalutamide did not block the estrogenic impact on respiration (Supplemental Figure S6C) nor the E_2-mediated increase in proliferation (Figure 6C), again demonstrating the specificity of the estrogenic response versus the AR signaling.

In addition, to reinforce the notion that the estrogen signaling pathway can bypass anti-androgen treatments, we also used a VCaP subline resistant to enzalutamide (formerly known as VCaP-ER (50), named herein VCaP-EnzR to avoid confusion). In these cells, and as observed in parental cells, there was an induction of mitochondrial respiration and cancer cell proliferation following E_2 exposure, demonstrating that the estrogen signaling pathway can conserve oncogenic functions even after the acquisition of EnzR (Supplemental Figure S6, D-E). The addition of the anti-estrogen fulvestrant impacted this hormonal regulation, but treatment with enzalutamide, blocking specifically AR, had no impact on the estrogenic response. We then used parental VCaP cells in xenograft assays to evaluate E_2's impact on PCa in an in vivo context. First, VCaP cells were injected in the flank of immunocompromised mice to allow tumor engraftment. When tumors became palpable, mice were castrated to ensure steroid deprivation. During surgery, hormone-

releasing pellets were also inserted subcutaneously, and mice were separated into two groups, receiving either a placebo or an E_2-releasing pellet. Importantly, in this context where no more androgens were in circulation, the presence of estrogens induced the growth of VCaP xenografts despite castration (Figure 6D). Furthermore, treatment with fulvestrant blocked the evolution of VCaP xenografted cells to surgical castration-resistance, despite the presence of E_2. Altogether, these findings confirm the oncogenic characteristics of the estrogen signaling pathway in PCa, independently of AR, and emphasize ERα's potential as a therapeutic target for patients with ERα-positive PCa.

To further support the clinical efficiency of SERMs in primary human PCa, we conducted, as a proof-of-principle, a pilot study using patient-derived organoids (PDOs) from prostate tumor tissues. In two PDO series, we observed a significant increase in organoid growth following E_2 treatment (Figure 6, E-F). Importantly, co-treatment with fulvestrant completely blocked this E_2-dependent growth. Interestingly, the PDO #2 line was originating from a patient that previously received neoadjuvant ADT prior to prostatectomy, thus suggesting that this PDO line could represent PCa transitioning to CRPC. In a third PDO line however, we observed no positive regulation of growth by E_2 (Figure 6, E-F). According to the differential response to E_2, *ESR1* transcript levels (ERα mRNA) were much higher in the E_2-responsive PDOs compared to the E_2-non-responsive PDO (Figure 6G). Moreover, to confirm that the impact of E_2 is indeed via the activation of ERα, we performed a knockdown experiment in an E_2-responsive PDO line using a doxycycline-inducible shRNA against *ESR1* (Supplemental Figure S6F). As such, the induction of growth by E_2 was abrogated following *ESR1* knockdown (Figure 6, H-I), further emphasizing the link between ERα expression and sensitivity to both E_2 and anti-estrogens in PCa cells.

With this vision of targeting ERα for therapeutic purposes, we then leveraged the TCGA PCa RNA-Seq dataset (30, 31). Based on the E_2-dependent signature obtained with human VCaP cells (presented in Figure 4), we designed an ERα-score that was applied to this RNA-Seq dataset (Figure 7A). Interestingly, most genes upregulated by E_2 in VCaP were also expressed at higher levels in patients with strong ERα-score, and vice-versa for E_2-dependent downregulated genes. Patients with high ERα-score, indicative of high transcriptional (metabolic) ERα signature, had a lower progression-free survival (Figure 7B). These results were further validated using the Taylor *et al.* (51) dataset, again demonstrating that patients with high ERα-scores had lower BCR-free survival (Figure 7C, and Supplemental Figure S6G). These results are in line with those shown in Figure 1, bridging ERα levels to its cancer-specific signature and PCa progression in patients.

Finally, we then wanted to assess if targeting ERα could also apply to patients with CRPC, as suggested by VCaP xenografts (Figure 6D). To this end, we reanalyzed RNA-Seq data from three published studies that investigated, in a small number of patients, the transcriptomic changes occurring before and after ADT (52-54). In the study from Shaw *et al.,* the *ESR1* gene expression had an 1.5-fold increase following ADT (adj. $p = 0.0002$), suggesting that *ESR1* is induced in cancer cells surviving ADT (Figure 7D). In line with this hypothesis, *ESR1* relative expression was also significantly induced in two other datasets post-ADT, by 3.1- and 4.4-fold (Figure 7, E-F, and Supplemental Figure S6, H-I). The ERα target gene *PGR* was also significantly increased in that context, supporting the hypothesis that both ERα expression and activity are increased during evolution to CRPC. In contrast, the *ESR2* gene, encoding for ERβ (see discussion), was barely detectable and did not change upon ADT. In a fourth RNA-Seq dataset comprised of 73 samples, *ESR1* and *PGR* were again significantly increased in tumor samples following ADT (Figure 7G). These analyses suggested that ERα activation could be linked to treatment resistance in CRPC.

Indeed, treatment with enzalutamide alone inhibited PDO growth, but E_2 stimulation was able to bypass this inhibition and still induce PDO growth (Figure 7, H-I). In line, in the Stand Up 2 Cancer (SU2C) RNA-Seq dataset, stronger ERα-score was observed in CRPC metastases, including lymph node and liver metastases, compared to localized tumors (Figure 7J) (55). Altogether, these results demonstrate that ERα transcriptional signature and expression are associated with PCa progression and resistance to treatments targeting the AR signaling pathway.

DISCUSSION

The current study demonstrates the heterogeneity of ERα protein levels in human PCa tumors, as well as the impact of ERα, when expressed, on disease progression. Mechanistically, transcriptomic analyses revealed that estrogens promote oncogenic and metabolic gene signatures in prostates of WT and PCa mouse models, as well as in ERα-positive VCaP cells. Accordingly, bioenergetic flux and metabolomics analyses confirmed metabolic regulation by estrogens. Consequently, E_2 treatment led to the positive regulation of proliferation and growth in VCaP cells (in vitro and in vivo) and PDOs that displayed ERα protein or mRNA expression. Conversely, this induced oncogenic phenotype was blocked by anti-estrogen and SERM treatments. Altogether, the current study demonstrates the role of ERα in promoting PCa cell proliferation and metabolism, as well as its potential to become a personalized therapeutic target for PCa.

Since the role of estrogens in the prostate and PCa was unclear, we first wanted to dissect the transcriptional functions of the estrogen signaling pathway using in vitro and in vivo preclinical models. In all the ERα-positive studied models, treatment with E_2 induced important transcriptional changes, mostly modulating genes associated with oncogenic pathways such as MYC and mTORC1, and promoted cancer cell metabolism, notably by increasing the expression of genes involved in mitochondrial respiration. Importantly, these experiments showed significant overlap in biological pathways modulated by both the androgen and the estrogen response. Indeed, AR is a well-known regulator of the mTORC1 signaling pathways, as well as an important modulator of PCa cell metabolism, notably by promoting mitochondrial biogenesis and activity (3, 4, 56). AR was shown to fuel mitochondrial respiration through pyruvate usage by regulating the mitochondrial pyruvate carrier gene *MPC2* (57). Herein, this androgen-dependent modulation of mitochondrial activity was also observed in normal and tumoral contexts, along with positive regulation by E_2, which highlights the estrogen signaling pathway as a new key orchestrator of

prostate and PCa cell metabolism. One of the important pathways induced by estrogens was OXPHOS, evidenced by transcriptional signatures and changes in mitochondrial respiration. Altogether, our results demonstrate that estrogens promote a specific transcriptional profile in PCa, with both distinct and overlapping genes compared to androgens and with most of their regulated functions similar to those regulated by AR. We thus believe that the activation of ERα partially mimics the action of androgens and, consequently, promotes PCa cell proliferation and disease progression.

Despite having been studied for decades, the effectiveness of anti-estrogen therapies in the context of PCa is still unclear. We believe this could be partly explained by the lack of accurate assessment of ERα expression status in prostate tumor cells before treatment administration. Indeed, in the breast cancer field, ERα protein levels are first evaluated in tumors to determine if they belong to ERα-positive or -negative subtypes, and this analysis then dictate the adequate treatment. Herein, using a clinically validated antibody, several tumors appeared to be ERα-negative, as previously reported (21), while other tumors showed positive ERα nuclear staining. This approach could be easily implemented in the clinical setting for PCa prognostication and treatment since it is routinely performed for breast cancer. Thus, by assessing ERα subtypes, we believe that this will allow the selection of patients with PCa that will have maximal chances to respond to anti-estrogenic therapies. Given that molecules targeting ERα have already been approved for ERα-positive breast cancer and other various clinical indications, if our hypothesis is validated in prospective clinical studies, stratifying PCa by ERα status to repurpose anti-estrogens could lead to additional therapeutic options in the PCa clinical landscape.

Since ERβ is also expressed in the prostate, we cannot rule out that some of the transcriptional changes observed in vivo are ERβ-dependent and not ERα-dependent. Based on work with βERKO mice, it is often thought that ERβ plays a tumor suppressor role (45). However,

this point is still controversial as other research groups, using slightly different mouse models, did not observe this relationship between ERβ and PCa (58-61). Future work is still required to fully dissect the prostate-specific response to E_2 and the functional interaction between ERα and ERβ. Herein, as most pathways transcriptionally regulated by E_2 were associated with oncogenic functions, and since we observed barely to no detectable levels of ERβ/*Esr2* in our models, we believe they are mostly regulated by ERα. Moreover, in two out of three different datasets where *ESR2* expression was investigated, there were no significant changes post-ADT in patients, as opposed to a significant increase in *ESR1* relative expression (Figure 7, E-G). These data also highlighted very little expression of *ESR2* in PCa tumors, further confirming that the changes observed following estrogen stimulation in our different models are induced by ERα activation.

Indeed, we have used several genetic and pharmacological tools to ensure that the estrogenic response was specific to ERα. These included siRNAs, an shRNA, and cells that do not express ERα (similar to a knockout). ERα-positive models included the mouse normal and tumoral prostate, parental VCaP and VCaP-EnzR cells, and some PDO lines, while ERα-negative models included PCa cell lines such as 22Rv1 and DU145, as well as one PDO line. The E_2-dependent transcriptional, metabolic, and pro-proliferative functions were observed in ERα-positive models, but not in ERα-negative models. The only exception was LNCaP cells, an ERα-negative cell line but with a mutated AR that can bind to E_2 (but not to PPT; Figure S6). For pharmacological tools, we used the specific ERα ligand PPT, as well as tamoxifen, raloxifene, toremifene, and fulvestrant, molecules that have been well characterized in vitro and in vivo in patients. Most of these molecules exhibit distinct structures (Supplemental Figure S7). The combination of several ligands (notably the ERα-specific agonist PPT) with distinct molecular structures all leading to the same conclusions further support the ERα-specific functions. Overall, using various approaches and models, we clearly demonstrated that the activation of the estrogen signaling pathway, and the beneficial

effects of targeting this pathway in preclinical models, is always observed in an ERα-dependent manner.

Altogether, the results presented herein emphasize the need to perform new clinical studies using molecules targeting the estrogen signaling pathway specifically in ERα-positive tumors. We believe that these molecules would be beneficial for both castration-sensitive and castration-resistant PCa, notably in combination with ADT and/or anti-androgens. Several lines of evidence support this hypothesis. First, the TMA with tumors from patients that received several rounds of treatments targeting AR, such as anti-androgens, before surgery. In this cohort, the active form of ERα (nuclear ERα) was associated with metastases and death following several years of ADT, thus clearly linking ERα signaling in the context of ADT and lethal CRPC. Secondly, results from Figure 7, comprising four different clinical datasets, show that ADT increases the expression levels of *ESR1*, encoding for ERα. These results support that ERα is indeed highly relevant during PCa treatment and evolution toward CRPC, as does the ER-score enrichment in castration-resistant metastases and VCaP xenograft's growth induced by E_2 in castrated mice. Thirdly, using VCaP cells, which were isolated from a CRPC tumor, and one hormone-naïve ERα-positive PDO line, we show that E_2 can bypass AR signaling to promote proliferation, growth, and metabolism, even when the anti-androgen enzalutamide is present. These experiments demonstrate that, at least in preclinical models, ERα activity can bypass AR blockade. This is in line with results from our TMA's validation cohort with neoadjuvant ADT and from RNA-Seq data before and after ADT. Interestingly, in a recent multi-sample whole genome analysis, *ESR1* amplification was observed during the transition of cancer cells to metastatic CRPC (62), supporting our results. *ESR1* amplifications are rare (or even absent) in primary hormone-naïve PCa tumors on the cBioPortal from *The Cancer Genome Atlas* consortium, but *ESR1* amplification is detected in metastatic CRPC samples, further strengthening the link between the estrogen signaling pathway and PCa

progression following AR targeted treatments. Future clinical studies considering the ERα status are thus needed to maximize the potential of drug repurposing of SERMs and anti-estrogens for the treatment of PCa.

Overall, our study supports the clinical relevance of ERα as a potential therapeutic target for the management of ERα-positive PCa tumors. Given the availability of both ERα clinical-grade antibodies and ERα-targeted drugs, repurposing of SERMs and anti-estrogens could rapidly be tested in prospective clinical studies in combination with anti-androgens in PCa patients with progressive disease.

METHODS

All materials and methods can be found in the Supplemental Files.

Sex as a biological variable

We only studied biological males given that the prostate is specific to biological males.

Statistics

For all details regarding statistics, please refer to the Supplemental Files. In brief, a *p*-value of 0.05, or an adjusted *p*-value for multiple testing of 0.05, were considered significant. When comparing two groups, Student's *t*-test was used (2-tailed). When comparing three groups or more, 1-way ANOVA was used with Dunnett (referring to one control group) or Tukey (comparing several groups) analyses. For survival analyses, the log-rank and Cox regression analyses were performed.

Study approval

All human and animal studies were approved by the appropriate institutional review boards. For PDO, written informed consent from patients was received before participation to the project CRCHUQ-UL (2021-5661). For mouse work, the study was approved by the Université Laval Research and Ethic Animal Committee (CHU-22-1206) at Quebec City (Canada).

Data availability

In vivo and in vitro RNA-Seq datasets generated for the current study are available on the Gene Expression Omnibus (GSE254635 and GSE256370). Other data can be found in the "Supporting data values" file, available in supplemental, or by contacting the corresponding author.

AUTHOR CONTRIBUTION

EAW designed the study. CL, LG, GHCS, CW, LB, HH, HB, CJ, LFP, RC, KG, AL, PC, CM, CB, MP, and EAW conducted experiments, acquired data, and provided reagents. HH, HB, CA, JR, ELa, AB, PT, CG, YF, FP, LL, and ELe acquired human tissues for TMA and PDO analyses. CL and EAW analyzed data, designed figures, and wrote the manuscript. All authors reviewed and approved the manuscript.

ACKNOWLEDGEMENTS AND GRANT SUPPORTS

This work was supported by funding to EAW from the Canadian Institutes for Health Research (CIHR; PJT159530) and the Canada Foundation for Innovation (CFI; #38622). CL, LFP, and KG were supported by a CIHR scholarship. LG, GHCS, CJ, and AL were supported by a scholarship from the Fonds de Recherche du Québec – Santé (FRQS). MP was supported by the CFI (#33805). MP is a Junior 2 scholar from the Fonds de recherche du Québec-Santé (FRQS). Ele was the recipient of a Prostate Cancer Canada rising star award (RS2013-55) and holder of a CIHR clinician-scientist phase II salary award. EAW holds a Tier 2 Canada Research Chair from the CIHR in targeting metabolic vulnerabilities for the treatment of hormone-sensitive cancers.

REFERENCES

1. Sung H, et al. Global Cancer Statistics 2020: GLOBOCAN Estimates of Incidence and Mortality Worldwide for 36 Cancers in 185 Countries. *CA Cancer J Clin.* 2021;71(3):209-49.
2. Germain L, et al. Preclinical models of prostate cancer - modelling androgen dependency and castration resistance in vitro, ex vivo and in vivo. *Nat Rev Urol.* 2023;20(8):480-93.
3. Gonthier K, et al. Functional genomic studies reveal the androgen receptor as a master regulator of cellular energy metabolism in prostate cancer. *Journal of Steroid Biochemistry and Molecular Biology.* 2019;17(8):1699-1709.
4. Audet-Walsh E, et al. Nuclear mTOR acts as a transcriptional integrator of the androgen signaling pathway in prostate cancer. *Genes & Development.* 2017;31(12):1228-42.
5. Zoubeidi A, and Ghosh PM. Celebrating the 80th anniversary of hormone ablation for prostate cancer. *Endocrine-Related Cancer.* 2021;28(8):T1-T10.
6. Smith MR, et al. Apalutamide Treatment and Metastasis-free Survival in Prostate Cancer. *New England Journal of Medicine.* 2018;378(15):1408-18.
7. Lafront C, et al. A Systematic Study of the Impact of Estrogens and Selective Estrogen Receptor Modulators on Prostate Cancer Cell Proliferation. *Scientific Reports.* 2020;10(1):4024.
8. Bonkhoff H. Estrogen receptor signaling in prostate cancer: Implications for carcinogenesis and tumor progression. *Prostate.* 2018;78(1):2-10.
9. Boibessot C, and Toren P. Sex steroids in the tumor microenvironment and prostate cancer progression. *Endocrine-Related Cancer.* 2018;25(3):R179-R96.
10. Ricke WA, et al. Prostatic hormonal carcinogenesis is mediated by in situ estrogen production and estrogen receptor alpha signaling. *Faseb Journal.* 2008;22(5):1512-20.

11. Walsh PC, and Wilson JD. The induction of prostatic hypertrophy in the dog with androstanediol. 1976;57(4):1093-7.

12. Bosland MC, et al. Induction at High Incidence of Ductal Prostate Adenocarcinomas in NBL/Cr and Sprague-Dawley Hsd:SD Rats Treated With a Combination of Testosterone and estradiol-17 Beta or Diethylstilbestrol. *Carcinogenesis.* 1995;16(6):1311-7.

13. Hu WY, et al. Estrogen-Initiated Transformation of Prostate Epithelium Derived from Normal Human Prostate Stem-Progenitor Cells. *Endocrinology.* 2011;152(6):2150-63.

14. McPherson SJ, et al. Elevated androgens and prolactin in aromatase-deficient mice cause enlargement, but net malignancy, of the prostate gland. *Endocrinology.* 2001;142(6):2458-67.

15. Bosland M, and Mahmoud A. Hormones and prostate carcinogenesis: Androgens and estrogens. *Journal of carcinogenesis.* 2011;10:33.

16. Salonia A, et al. Circulating Estradiol, But Not Testosterone, Is a Significant Predictor of High-Grade Prostate Cancer in Patients Undergoing Radical Prostatectomy. *Cancer.* 2011;117(22):5029-38.

17. Toren P, et al. Serum Sex Steroids as Prognostic Biomarkers in Patients Receiving AndrogenDeprivation Therapy for Recurrent Prostate Cancer: A Post Hoc Analysis of the PR.7 Trial. *Clinical Cancer Research.* 2018;24(21):5305-12.

18. McPherson SJ, et al. Estrogen receptor-beta activated apoptosis in benign hyperplasia and cancer of the prostate is androgen independent and TNF alpha mediated. *Proceedings of the National Academy of Sciences of the United States of America.* 2010;107(7):3123-8.

19. Mak P, et al. Prostate Tumorigenesis Induced by PTEN Deletion Involves Estrogen Receptor beta Repression. *Cell Reports.* 2015;10(12):1982-91.

20. Warner M, et al. 25 years of ER beta: a personal journey. *Journal of Molecular Endocrinology.* 2022;68(1):R1-R9.

21. Takizawa I, et al. Estrogen receptor alpha drives proliferation in PTEN-deficient prostate carcinoma by stimulating survival signaling, MYC expression and altering glucose sensitivity. *Oncotarget.* 2015;6(2):604-16.

22. Furic L, et al. Pro-tumorigenic role of ER alpha in prostate cancer cells. *Aging-Us.* 2015;7(6):356-7.

23. Katzenellenbogen JA, et al. Structural underpinnings of oestrogen receptor mutations in endocrine therapy resistance. *Nature Reviews Cancer.* 2018;18(6):377-88.

24. Fujimura T, et al. Toremifene, a selective estrogen receptor modulator, significantly improved biochemical recurrence in bone metastatic prostate cancer: a randomized controlled phase II a trial. *BMC Cancer.* 2015;15:836.

25. Steiner MS and Pound CR. Phase IIA clinical trial to test the efficacy and safety of Toremifene in men with high-grade prostatic intraepithelial neoplasia. 2003;2(1):24-31.

26. Price D, et al. Toremifene for the prevention of prostate cancer in men with high grade prostatic intraepithelial neoplasia: Results of a double-blind, placebo controlled, phase IIB clinical trial. *Journal of Urology.* 2006;176(3):965-70.

27. Stein S, et al. Phase II trial of toremifene in androgen-independent prostate cancer - A Penn cancer clinical trials group trial. *American Journal of Clinical Oncology-Cancer Clinical Trials.* 2001;24(3):283-5.

28. Taneja SS, et al. Prostate Cancer Diagnosis Among Men With Isolated High-Grade Intraepithelial Neoplasia Enrolled Onto a 3-Year Prospective Phase III Clinical Trial of Oral Toremifene. *Journal of Clinical Oncology.* 2013;31(5):523-9.

29. Bergan RC, et al. A phase II study of high-dose tamoxifen in patients with hormone-refractory prostate cancer. *Clinical Cancer Research.* 1999;5(9):2366-73.

30. Gao J, et al. Integrative analysis of complex cancer genomics and clinical profiles using the cBioPortal. *Sci Signal.* 2013;6(269):pl1.

31. Cerami E, et al. The cBio cancer genomics portal: an open platform for exploring multidimensional cancer genomics data. *Cancer Discov.* 2012;2(5):401-4.

32. Belledant A, et al. The UGT2B28 Sex-steroid Inactivation Pathway Is a Regulator of Steroidogenesis and Modifies the Risk of Prostate Cancer Progression. *European Urology.* 2016;69(4):601-9.

33. Lacombe L, et al. UGT2B28 accelerates prostate cancer progression through stabilization of the endocytic adaptor protein HIP1 regulating AR and EGFR pathways. *Cancer Letters.* 2023;553:215994.

34. Gevaert T, et al. The potential of tumour microenvironment markers to stratify the risk of recurrence in prostate cancer patients. *PLoS One.* 2020;15(12):e0244663.

35. Gangkak G, et al. Immunohistochemical analysis of estrogen receptors in prostate and clinical correlation in men with benign prostatic hyperplasia. *Investig Clin Urol.* 2017;58(2):117-26.

36. Sehgal PD, et al. Tissue-specific quantification and localization of androgen and estrogen receptors in prostate cancer. *Hum Pathol.* 2019;89:99-108.

37. Pihlajamaa P, et al. Tissue-specific pioneer factors associate with androgen receptor cistromes and transcription programs. *EMBO J.* 2014;33(4):312-26.

38. Karthaus WR, et al. Regenerative potential of prostate luminal cells revealed by single-cell analysis. *Science.* 2020;368(6490):497-505.

39. Qiu XT, et al. MYC drives aggressive prostate cancer by disrupting transcriptional pause release at androgen receptor targets. *Nature Communications.* 2022;13(1):2559.

40. Liberzon A, et al. The Molecular Signatures Database Hallmark Gene Set Collection. *Cell Systems.* 2015;1(6):417-25.

41. Nishi K, et al. Novel estrogen-responsive genes (ERGs) for the evaluation of estrogenic activity. *Plos One.* 2022;17(8):e0273164.

42. Messier TL, et al. Epigenetic and transcriptome responsiveness to ER modulation by tissue selective estrogen complexes in breast epithelial and breast cancer cells. *PLoS One.* 2022;17(7):e0271725.

43. Wang SY, et al. Prostate-specific deletion of the murine Pten tumor suppressor gene leads to metastatic prostate cancer. *Cancer Cell.* 2003;4(3):209-21.

44. Nelson AW, et al. Comprehensive assessment of estrogen receptor beta antibodies in cancer cell line models and tissue reveals critical limitations in reagent specificity. *Molecular and Cellular Endocrinology.* 2017;440I:138-50.

45. Gustafsson JA, et al. Update on ERbeta. *Journal of Steroid Biochemistry and Molecular Biology.* 2019;191:105312.

46. Korenchuk S, et al. VCaP, a cell-based model system of human prostate cancer. *In Vivo.* 2001;15(2):163-8.

47. Chakravarty D, et al. The oestrogen receptor alpha-regulated lncRNA NEAT1 is a critical modulator of prostate cancer. *Nature Communications.* 2014;5:5383.

48. Andrzejewski S, et al. Metformin directly acts on mitochondria to alter cellular bioenergetics. *Cancer Metab.* 2014;2:12.

49. Audet-Walsh E, et al. SREBF1 Activity Is Regulated by an AR/mTOR Nuclear Axis in Prostate Cancer. *Mol Cancer Res.* 2018;16(9):1396-405.

50. Lelong EIJ, et al. Prostate cancer resistance leads to a global deregulation of translation factors and unconventional translation. *NAR Cancer.* 2022;4(4):zcac034.

51. Taylor BS, et al. Integrative genomic profiling of human prostate cancer. *Cancer Cell.* 2010;18(1):11-22.

52. Shaw GL, et al. The Early Effects of Rapid Androgen Deprivation on Human Prostate Cancer. *Eur Urol.* 2016;70(2):214-8.

53. Rajan P, et al. Next-generation sequencing of advanced prostate cancer treated with androgen-deprivation therapy. *Eur Urol.* 2014;66(1):32-9.

54. Rajan P, et al. Identification of a candidate prognostic gene signature by transcriptome analysis of matched pre- and post-treatment prostatic biopsies from patients with advanced prostate cancer. *BMC Cancer.* 2014;14:977.

55. Abida W, et al. Genomic correlates of clinical outcome in advanced prostate cancer. *Proc Natl Acad Sci U S A.* 2019;116(23):11428-36.

56. Pulliam TL, et al. Regulation and role of CAMKK2 in prostate cancer. *Nature Reviews Urology.* 2022;19(6):367-80.

57. Bader DA, et al. Mitochondrial pyruvate import is a metabolic vulnerability in androgen receptor-driven prostate cancer. *Nat Metab.* 2019;1(1):70-85.

58. Antal MC, et al. Sterility and absence of histopathological defects in nonreproductive organs of a mouse ERbeta-null mutant. *Proc Natl Acad Sci U S A.* 2008;105(7):2433-8.

59. Dupont S, et al. Effect of single and compound knockouts of estrogen receptors alpha (ERalpha) and beta (ERbeta) on mouse reproductive phenotypes. *Development.* 2000;127(19):4277-91.

60. Prins GS, et al. Estrogen imprinting of the developing prostate gland is mediated through stromal estrogen receptor alpha: studies with alphaERKO and betaERKO mice. *Cancer Res.* 2001;61(16):6089-97.

61. Krege JH, et al. Generation and reproductive phenotypes of mice lacking estrogen receptor beta. *Proc Natl Acad Sci U S A.* 1998;95(26):15677-82.

62. Nurminen A, et al. Cancer origin tracing and timing in two high-risk prostate cancers using multisample whole genome analysis: prospects for personalized medicine. *Genome Med.* 2023;15(1):82.

FIGURE LEGENDS

Figure 1

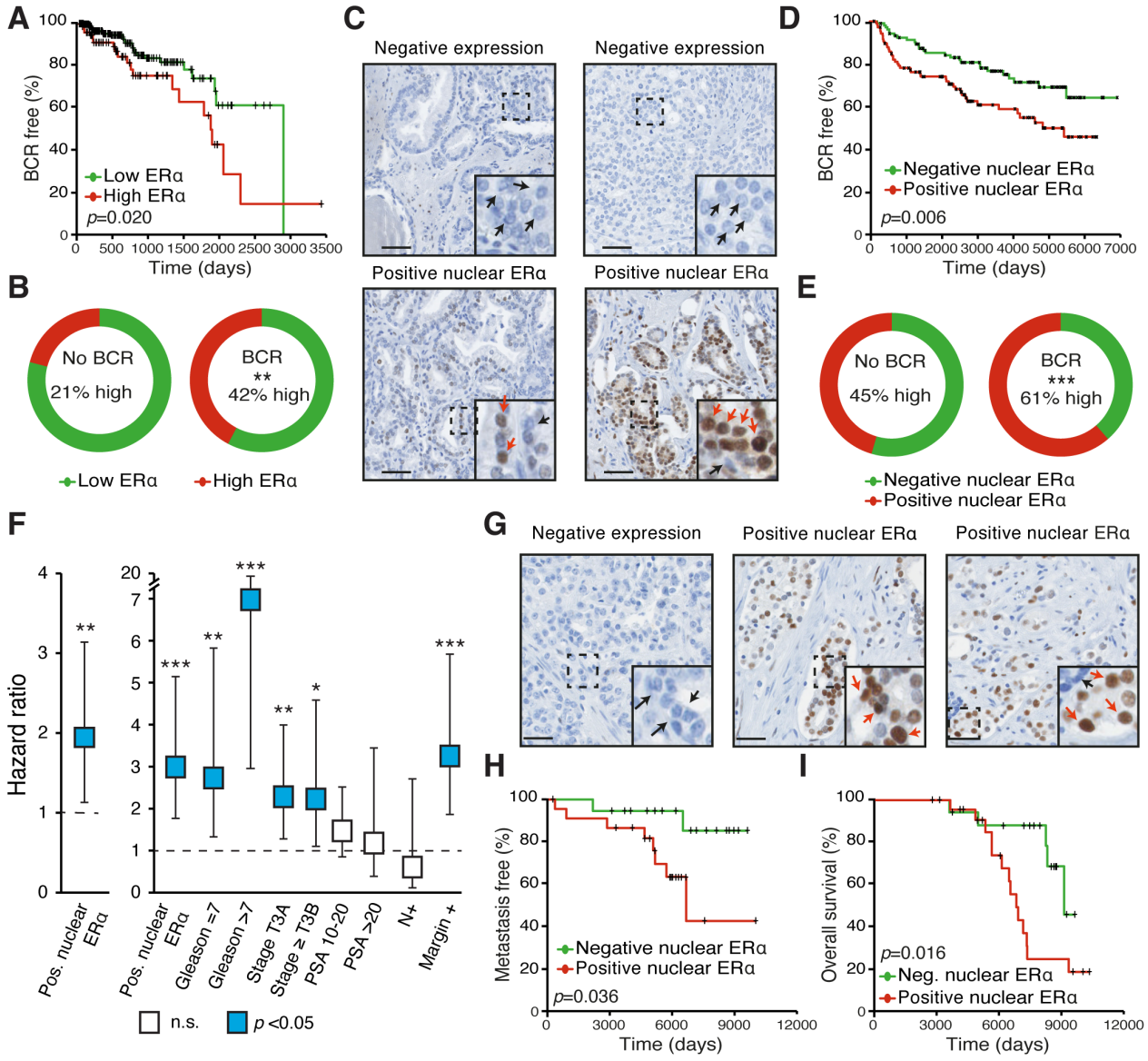

Figure 1. ERα expression is heterogenous in PCa and, when nuclear (active), is associated with biochemical recurrence (BCR). (**A**) Kaplan-Meier of BCR-free survival following radical prostatectomy in patients from the TCGA-PRAD cohort with high or low ERα protein expression levels (no distinction between nuclear and cytoplasmic localization). (**B**) Proportions of patients with high or low ERα protein expression levels, with and without BCR, from the TCGA cohort (**p<0.0019, Chi-square test). (**C-F**) Analysis of the Belledant *et al.* (32) cohort. (**C**)

Representative images of ERα immunohistochemistry in four PCa patients. Black and red arrows respectively highlight negative and positive staining. Scale = 50 μm. (**D**) Kaplan-Meier BCR-free survival following radical prostatectomy in patients with positive versus negative ERα nuclear levels. (**E**) Proportions of patients with positive or negative ERα nuclear levels, with and without BCR, from the TMA cohort (***p<0.001, Chi-square test). (**F**) Cox regression analyses of the impact of positive (Pos.) nuclear ERα levels on the risk of BCR, with *p< 0.05, **p<0.01 and ***p<0.001. Boxes illustrate hazard ratios with their respective 95% confidence intervals. Results are shown without (left) and with (right) additional BCR risk factors. Reference groups for covariables: Gleason score of 6; Stage of T2C and below; prostate-specific antigen (PSA) pre-surgery levels under 10 ng/mL; negative lymph node invasion and negative margins. n.s. = non-significant. (**G-I**) Analysis of an independent cohort of patients that received neoadjuvant hormonotherapy before surgery. (**G**) Representative images of ERα immunohistochemistry in four PCa patients. Black and red arrows respectively highlight negative and positive staining. Scale = 50 μm. (**H** and **I**) Kaplan-Meier survival analysis in patients with positive versus negative ERα nuclear levels regarding the development of metastasis (**H**) and overall survival (**I**). For Kaplan-Meier survival curves, the log-rank test p-value is shown inset.

Figure 2

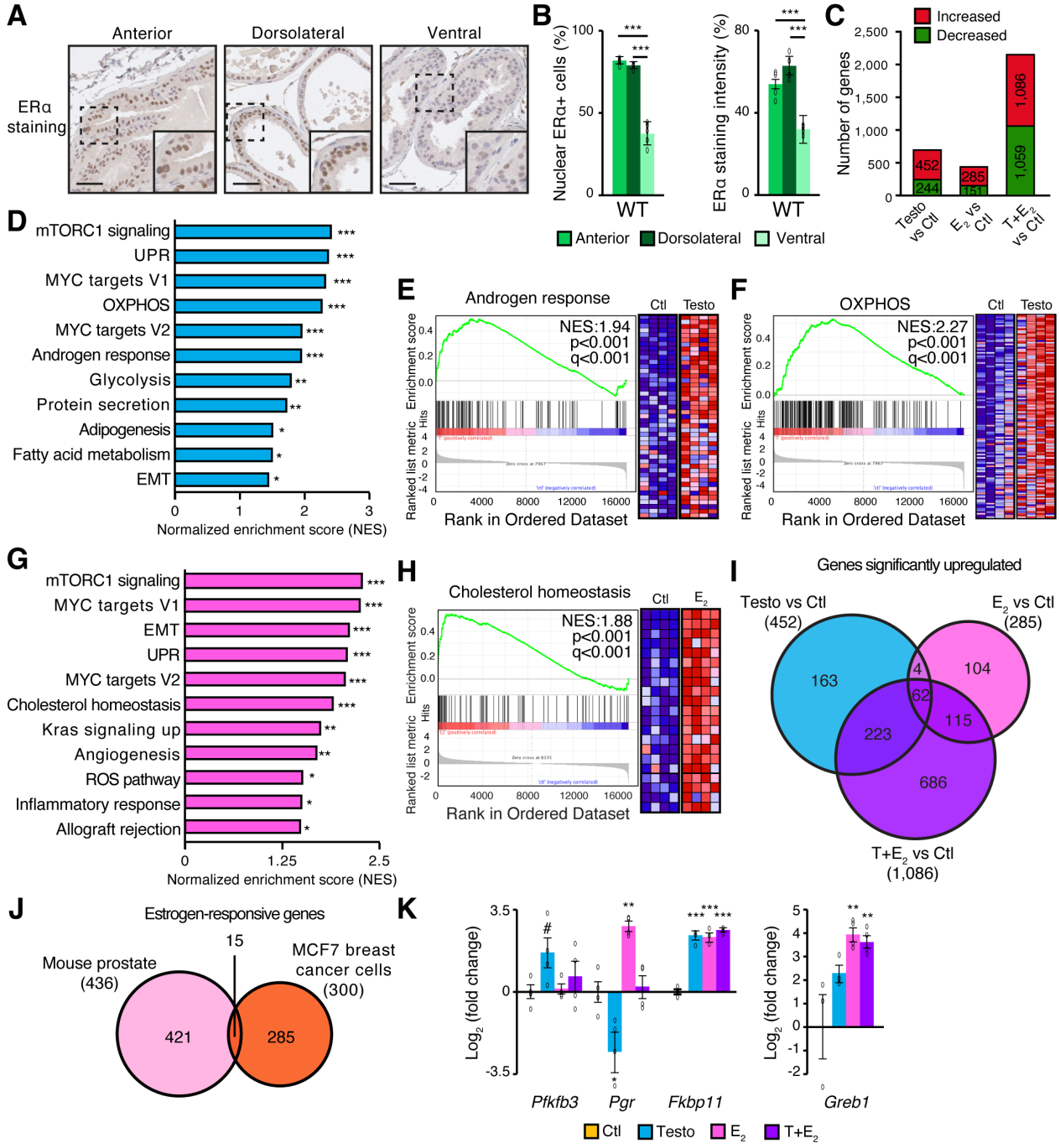

Figure 2. Estrogens modulate the normal prostate transcriptome in vivo, activating oncogenic pathways similar to androgen stimulation. (**A**) Representative images of immunohistochemistry of ERα in the normal mouse prostate lobes. Scale = 50 μm. (**B**) Quantification of ERα-positive and of ERα staining intensity in the normal mouse prostate lobes (~2,700 cells/animal, 5

animals/lobe). (**C**-**I**) RNA-Seq analyses of the murine prostate transcriptome 24h following injections with vehicle (Ctl), testosterone (Testo), estradiol (E_2), or both (T+E_2). Mice were castrated three days before injections to ensure hormonal deprivation. (**C**) Number of significantly differentially expressed genes following pair-wise comparisons between conditions. Thresholds used were a fold-change ≥ 1.75 or ≤ -1.75 and a *p*-value with FDR < 5%. (**D**) Normalized enrichment scores (NES) of Gene Set Enrichment Analysis (GSEA) following treatment with testosterone. (**E** and **F**) GSEA diagrams and heatmaps for the androgen response (**E**) and the oxidative phosphorylation (OXPHOS) (**F**) gene sets following testosterone treatment in vivo. (**G**) NES of GSEA analysis enriched following E_2 treatment in vivo. (**H**) GSEA diagram and heatmap for the cholesterol homeostasis gene set following E_2 treatment. For (**E**, **F** and **H**), NES, *p*-values and *q*-values are indicated on each diagram and only core genes of each pathway are shown. For (**D** and **G**), **q* < 0.05, ***q* < 0.01 and ****q* < 0.001 in GSEA. (**I**) Venn diagram of upregulated genes for each pair-wise comparison. (**J**) Venn diagram of estrogen-responsive genes in breast cancer cells (MCF7), using the dataset from (41), and in the mouse prostate. Circle and overlap sizes are not proportional to the number of genes. (**K**) qRT-PCR of positive controls for androgenic (*Pfkfb3* and *Fkbp11*) and estrogenic regulation (*Pgr, Fkbp11* and *Greb1*). For (**B** and **K**), results are shown as the average with SEM with #*p*<0.010, **p*<0.05, and ****p*<0.001; *n*=4 mice/treatment; 1-way ANOVA).

Figure 3

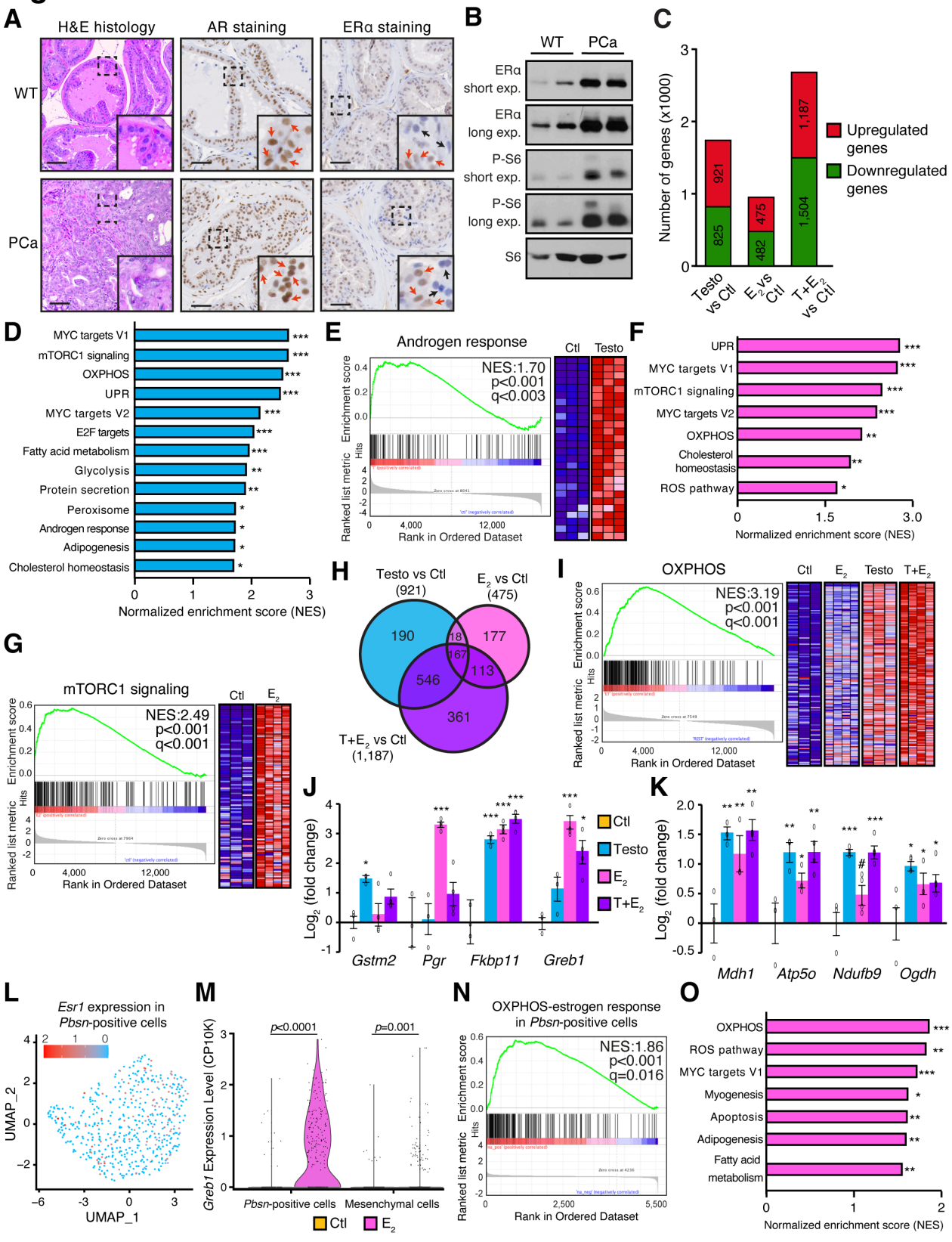
A
H&E histology
AR staining
ERα staining
WT
PCa
B
WT
PCa
ERα short exp.
ERα long exp.
P-S6 short exp.
P-S6 long exp.
S6
C
Number of genes (x1000)
Upregulated genes
Downregulated genes
921
825
475
482
1,187
1,504
Testo vs Ctl
E2 vs Ctl
T+E2 vs Ctl
D
MYC targets V1
mTORC1 signaling
OXPHOS
UPR
MYC targets V2
E2F targets
Fatty acid metabolism
Glycolysis
Protein secretion
Peroxisome
Androgen response
Adipogenesis
Cholesterol homeostasis
Normalized enrichment score (NES)
E
Androgen response
NES:1.70
p<0.001
q<0.003
Ctl
Testo
Enrichment score
Ranked list metric
Hits
Rank in Ordered Dataset
F
UPR
MYC targets V1
mTORC1 signaling
MYC targets V2
OXPHOS
Cholesterol homeostasis
ROS pathway
Normalized enrichment score (NES)
G
mTORC1 signaling
NES:2.49
p<0.001
q<0.001
Ctl
E2
Enrichment score
Ranked list metric
Hits
Rank in Ordered Dataset
H
Testo vs Ctl (921)
E2 vs Ctl (475)
T+E2 vs Ctl (1,187)
190
18
177
167
113
546
361
I
OXPHOS
NES:3.19
p<0.001
q<0.001
Ctl
E2
Testo
T+E2
Enrichment score
Ranked list metric
Hits
Rank in Ordered Dataset
J
Log2 (fold change)
Ctl
Testo
E2
T+E2
Gstm2
Pgr
Fkbp11
Greb1
K
Log2 (fold change)
Mdh1
Atp5o
Ndufb9
Ogdh
L
Esr1 expression in Pbsn-positive cells
UMAP_2
UMAP_1
M
p<0.0001
p=0.001
Greb1 Expression Level (CP10K)
Pbsn-positive cells
Mesenchymal cells
Ctl
E2
N
OXPHOS-estrogen response in Pbsn-positive cells
NES:1.86
p<0.001
q=0.016
Enrichment score
Ranked list metric
Hits
Rank in Ordered Dataset
O
OXPHOS
ROS pathway
MYC targets V1
Myogenesis
Apoptosis
Adipogenesis
Fatty acid metabolism
Normalized enrichment score (NES)

Figure 3. Estrogens activate oncogenic pathways in a PCa mouse model. (**A**) Representative images of Hematoxylin and Eosin (H&E; left) and staining of AR and ERα in prostates from 24-week-old WT and PCa-developing mice. Black and red arrows respectively highlight negative and positive staining. Scale = 50 µm. (**B**) Western blot of prostates from WT and PCa-developing mice. P-S6 shows activation of the mTOR signaling following prostate-specific deletion of *Pten* in tumors. S6 = loading control. (**C**-**I**) RNA-Seq analyses of mouse PCa tumors following 24h treatment in vivo with vehicle (Ctl), testosterone (Testo), estradiol (E_2), or both ($T+E_2$). Mice were castrated three days before injections to ensure steroid deprivation. (**C**) Number of differentially expressed genes following pair-wise comparisons. (**D** and **F**) Normalized enrichment scores (NES) of Gene Set Enrichment Analysis (GSEA) following treatment with Testo (**D**) or E_2 (**F**), with *q<0.05, **q< 0.01 and ***q<0.001. (**E**, **G** and **H**) GSEA diagrams and heatmaps for the androgen response following Testo treatment (**E**), the mTORC1 gene set following E_2 treatment (**G**), and the OXPHOS gene set following $T+E_2$ treatment (**I**). Only core genes are shown. (**H**) Venn diagrams of upregulated genes for each pair-wise comparison. (**J** and **K**) qRT-PCR of positive controls (**J**) and metabolic genes (**K**) following treatments. Results are shown as the mean ± SEM (3-4 mice/condition). (**L**-**O**) Single-cell RNA-Seq analyses from tumoral murine prostates, with and without treatment with E_2 (2 mice/condition). (**L**) *Esr1* expression in *Pbsn*-positive epithelial cells (in log scale of [counts/10K [CP10K] + 1]). (**M**) *Greb1* expression in mesenchymal and epithelial-*Pbsn*-positive clusters. (**N** and **O**) NES of GSEA analysis enriched following E_2 treatment in *Pbsn*-positive epithelial cells (**O**), with the GSEA diagram for the OXPHOS gene set (**N**). Significance was calculated using 1-way ANOVA or a 2-tailed Student's *t*-test, with *p<0.05, **p<0.01 and ***p<0.001.

Figure 4

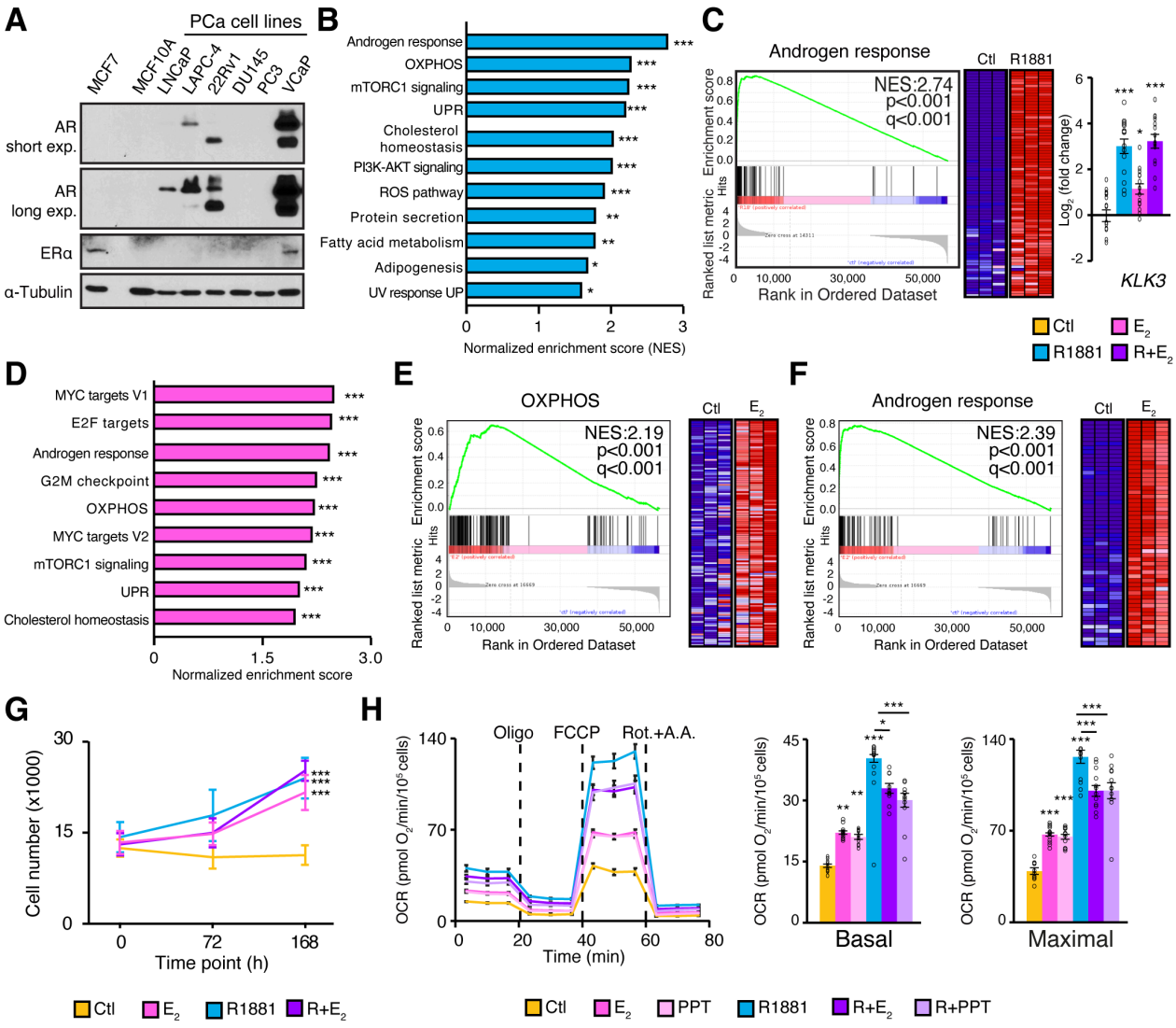

Figure 4. ERα transcriptional program promotes PCa cell metabolism and proliferation. (**A**) Western blot of AR and ERα in in vitro models: one ERα-positive breast cancer cell line (MCF7), one ERα-negative mammary gland cell line (MCF10A) and 6 human PCa cell lines (loading control = α-tubulin). (**B-F**) RNA-Seq analyses of VCaP cells following 24h treatment with vehicle (Ctl), the synthetic androgen R1881, estradiol (E_2), or both ($R+E_2$). (**B**) Normalized enrichment scores (NES) of Gene Set Enrichment Analysis (GSEA) following treatment with R1881. (**C, left**) GSEA diagrams and heatmaps for the androgen response gene set following treatment with R1881. (**C,**

right) qRT-PCR of *KLK3* expression, encoding prostate-specific antigen (PSA). Values are shown as average with SEM of four independent experiments performed in triplicates. (**D**) NES of GSEA analysis enriched following treatment with E_2. For (**B** and **D**), *$q < 0.05$, **$q < 0.01$ and ***$q < 0.001$. GSEA diagrams and heatmaps for the OXPHOS (**E**) and androgen response (**F**) gene sets following treatment with E_2 in VCaP cells. For (**C**, **E** and **F**), NES, *p*-values, and *q*-values are indicated on each diagram and only core genes of each pathway are shown. (**G**) VCaP proliferation assay following treatment with either R1881, E_2, or both. One representative experiment out of four independent experiments is shown. Results are shown as the mean ± SEM (n=6-8/treatment group). (**H**) VCaP oxygen consumption rates (OCR) profiles following 72h treatment with either R1881, E_2, or both. Complete mitochondrial stress test, with basal and maximal OCR capacities, are shown. One representative independent experiment out of three is shown. Results are shown as the mean of normalized data to cell numbers ± SEM (n=10–12/treatment). For (**C**, **G** and **H**), Significance was calculated using 1-way ANOVA **$p<0.01$ and ***$p<0.001$.

Figure 5

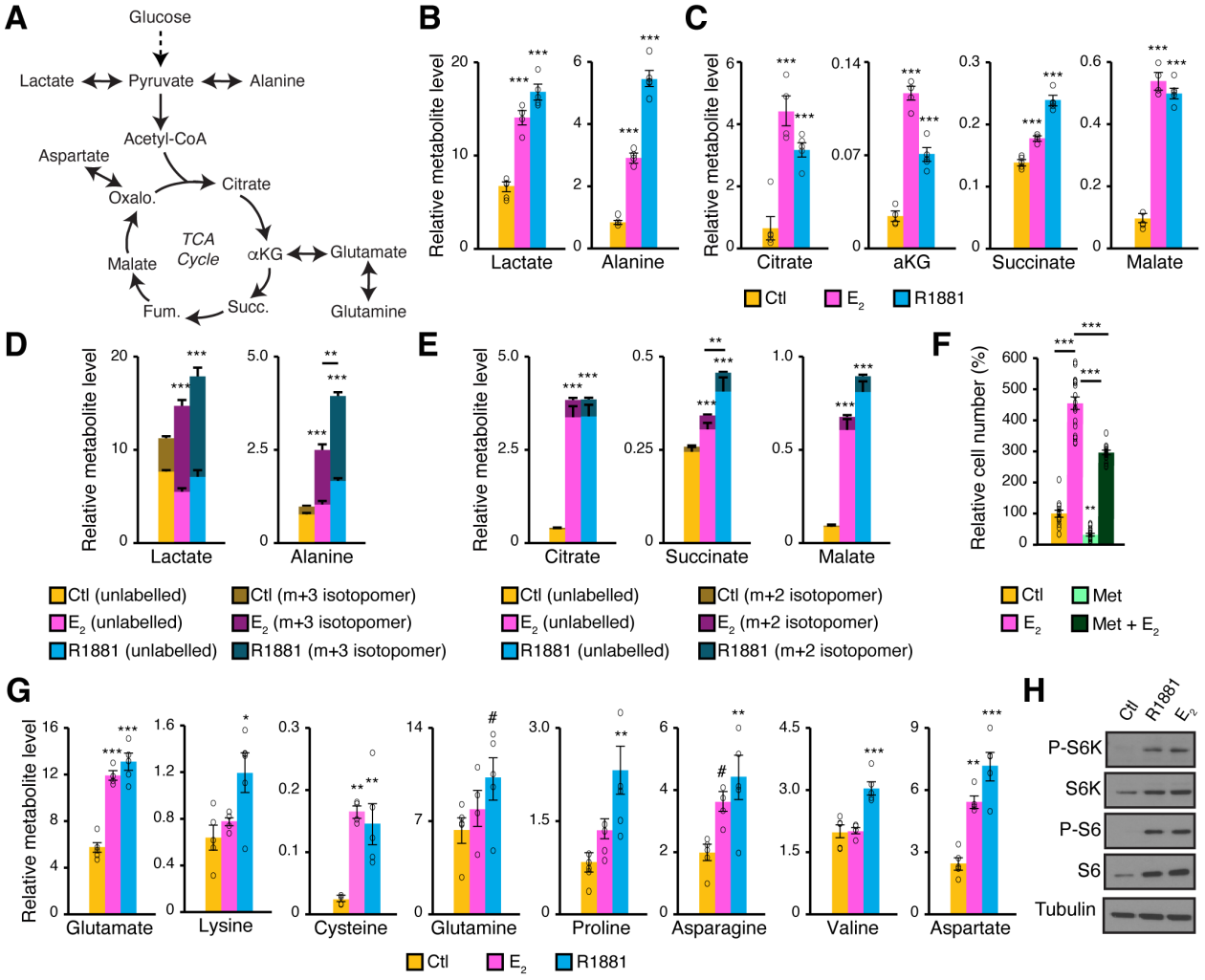

Figure 5. ERα activation induces cancer cell metabolism notably by promoting glucose consumption and usage. (**A**) Schematic overview of glucose metabolism through glycolysis to allow pyruvate synthesis, which can then fuel the mitochondrial TCA cycle for respiration. Note that not all enzymatic reactions are shown (dashed lines symbolize intermediate steps). (**B** and **C**) Quantification of lactate (**B, left**), alanine (**B, right**) and TCA cycle intermediates (**C**) in VCaP cells following 72h treatment with estradiol (E_2) or the synthetic androgen R1881 by gas chromatography-mass spectrometry (GC-MS). (**D** and **E**) Quantification of ^{13}C incorporation from ^{13}C-glucose in lactate (**D, left**), alanine (**D, right**) and TCA cycle intermediates (**E**) in VCaP cells

following 72h treatment with E_2 or R1881. ^{13}C-glucose allow enrichment in m+3 for lactate and alanine and m+2 for citrate, succinate, and malate if it feeds the TCA cycle. (**F**) Changes in VCaP cell number following 168h treatment with either E_2, the inhibitor of mitochondrial respiration metformin (Met), or both (Met + E_2). The changes in cell numbers were normalized in percentages according to the control treatment. Results are shown as the mean ± SEM of two independent experiments (n=16/treatment group). (**G**) Quantification of amino acids connected to energy synthesis pathways in VCaP cells following 72h treatment with E_2 or R1881 by GC-MS. For (**B**-**E** and **G**), results are shown as the mean ± SEM of one representative experiment (n=5/conditions) out of three independent experiments. (**H**) Western blot of mTOR signaling pathway, with phosphorylation of downstream targets (S6 and S6K) following hormonal treatment. α-tubulin was used as a loading control. *p<0.05, **p<0.01 and ***p<0.001 respective to control conditions or as indicated, using 1-way ANOVA. For (**D** and **E**), p-values are only shown for metabolites with ^{13}C labelling.

Figure 6

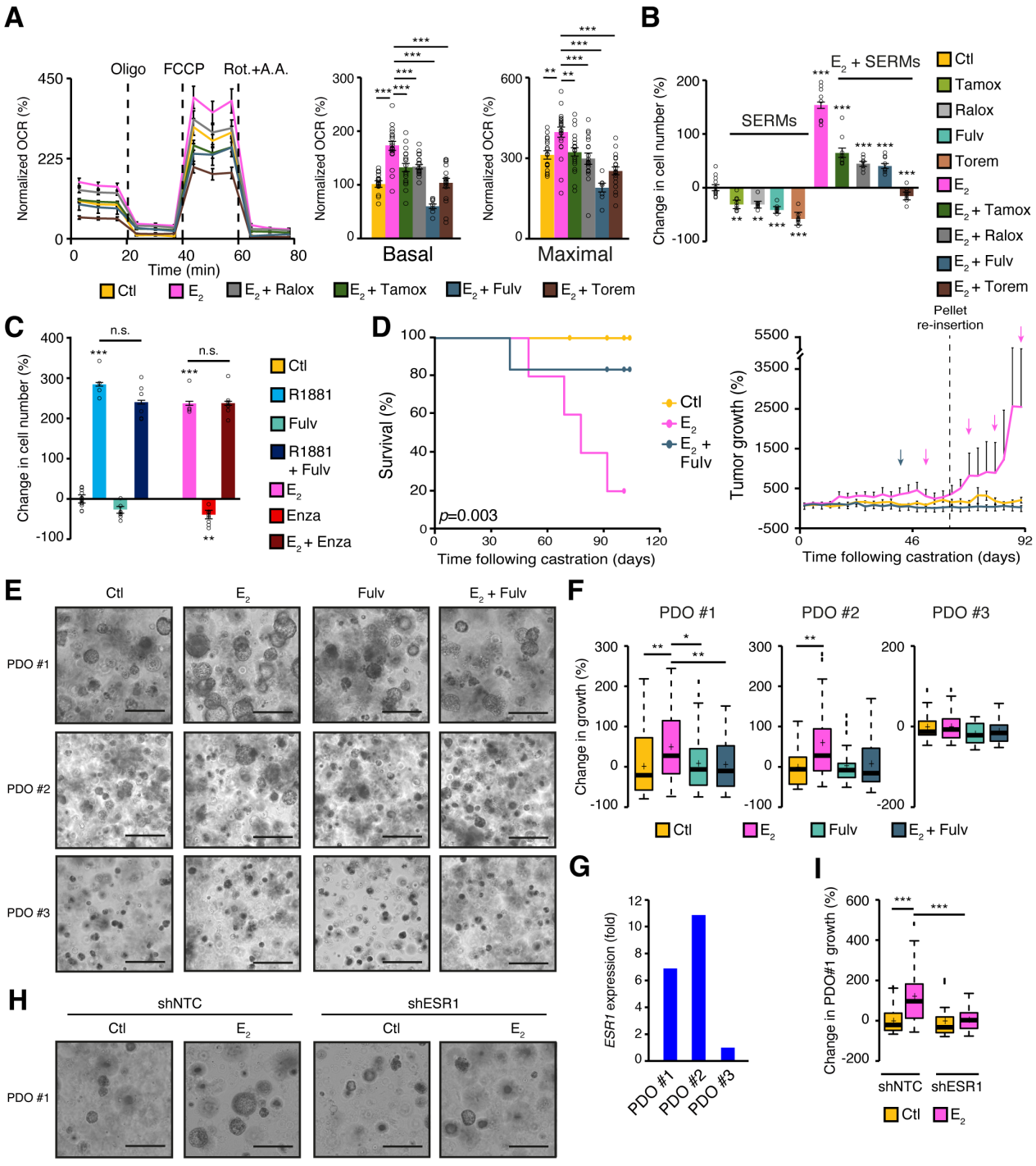

Figure 6. SERMs and fulvestrant inhibit the E_2-dependent induction in mitochondrial respiration, proliferation, and growth of PCa cells. (**A**) VCaP oxygen consumption rates (OCR) profiles following 72h treatment with estradiol (E_2), tamoxifen (Tamox), raloxifene (Ralox),

toremifene (Torem), and fulvestrant (Fulv). Complete mitochondrial stress test of one experiment is shown, with basal and maximal OCR capacities shown as the average of two out of three independent experiments (mean ± SEM (*n*=8-12/treatment per experiment). Changes in VCaP cell number following 168h treatment with anti-estrogens co-treated with E_2 (**B**), or with hormones co-treated with fulvestrant or enzalutamide (**C**), normalized to control. One representative experiment out of three independent experiments is shown (mean ± SEM; *n*=6-8/condition). (**D**) Kaplan-Meier of survival (left) and tumor growth (right) of castrated mice with VCaP xenografts, under either placebo or E_2 pellet, and injected weekly with either vehicle or fulvestrant (5-10 mice/condition). The log-rank test *p*-value is shown. Tumor volume was normalized to 100% based on size at castration. Tumor growth is shown up to 90 days, at which most E_2-treated tumors were harvested. Colored arrows indicate mice reaching ethical limit points. (**E** and **F**) Brightfield imaging (**E**) and changes of organoid growth (**F**) of three patient-derived organoid (PDO) lines after 14-15 days of treatment with vehicles, E_2, Fulv, or both. (**G**) qRT-PCR of *ESR1* in PDO lines shown in (**E**). Results are shown in fold change compared to PDO#3. (**H** and **I**) Brightfield imaging (**H**) and changes of organoid growth (**I**) of the PDO#1 after 15 days of treatment with vehicle and E_2, with and without *ESR1* knockdown. For (**E** and **H**), scale = 300 µm. For (**F** and **I**), results are shown as the mean ± SEM (*n*=4 replicates/condition. Significance was calculated using 1-way ANOVA; **p*< 0.05, ***p*<0.01 and ****p*<0.001.

Figure 7

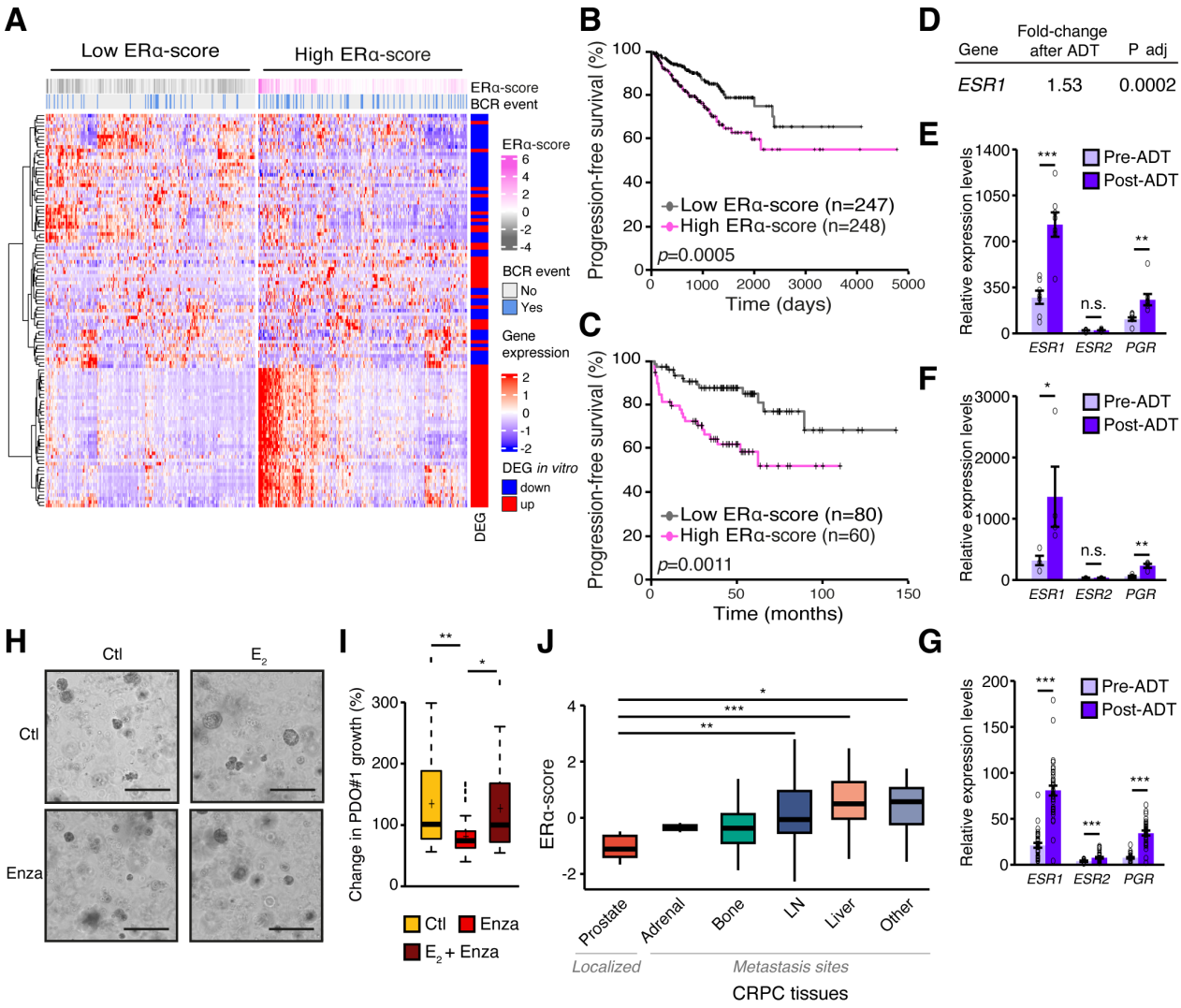

Figure 7. *ESR1* is increased following androgen deprivation therapy (ADT) and its transcriptional signature is associated with PCa progression. (**A**) Heatmap of the ERα gene signature in patients from the TCGA-PRAD dataset (30, 31). The ERα-score is the predicted transcriptional activity of ERα. BCR = biochemical recurrence. Legend shows differentially expressed genes (DEG) with increased (red) or decreased (blue) expression following estrogen (E_2) treatment in VCaP cells. (**B** and **C**) Kaplan-Meier of BCR-free survival following surgery in patients from the TCGA-PRAD (**B**) and the Taylor (**C**) datasets, separated between high and low ERα-score. Log-rank test *p*-values are shown. (**D**) *ESR1* (encoding for ERα) expression in PCa

tumors before and after androgen deprivation therapy (ADT) in the Eur Uro 2017 dataset (52). (**E**) *ESR1*, *ESR2*, and *PGR* gene expression in PCa tumors before and after ADT in the Eur Uro 2014 dataset (53) (n=7 paired samples). (**F**) *ESR1*, *ESR2* and *PGR* gene expression in PCa tumors before and after ADT+docetaxel in the BMC cancer dataset (54) (n=4 paired samples). (**G**) *ESR1*, *ESR2* and *PGR* gene expression in PCa tumors before and after ADT in the GSE183100 dataset (n=73 samples). (**H** and **I**) Brightfield imaging (scale = 300 μm) (**H**) and changes of organoid growth (**I**) of the patient-derived organoid (PDO) line #1 after treatment with vehicle (Ctl) and the anti-androgen enzalutamide (Enza) co-treated or not with E_2. (**J**) ERα-score in the Stand Up 2 Cancer (SU2C) dataset (55), separated by tumor localization: in the prostate (n=5), and metastases in either adrenal glands (n=2), bone (n=82), lymph nodes (LN; n=79), liver (n=26), and other sites (n=14). Significance was calculated using 1-way ANOVA or a 2-tailed Student's t-test, as appropriate; *p<0.05, **p<0.01 and ***p<0.001.